

**ARAŞTIRMA MAKALESİ / RESEARCH ARTICLE**

**FOCUSED ION BEAM FABRICATION OF ELECTROCHEMICALLY  
SYNTHESIZED NANOWIRE-BASED ELECTRODES**

**S. VALIZADEH<sup>1</sup>**

**ABSTRACT**

A new nanoelectrode device with a gap size of about 30 nm was fabricated using 200 nm in diameter electrochemically synthesized Au nanowire. The gap was created by Focused Ion Beam milling at  $10^{17}$  ions /  $\text{cm}^2$  and dwell time of 0.2  $\mu\text{s}$ . The I-V characterization of the circuit prior to FIB milling and of the empty gap circuit in air showed the resistances of 0.55 M $\Omega$  and 4 G $\Omega$ , respectively.

**Keywords :** Template synthesis; Focused ion beam; Nano electrode; Au nanowire; Nanogap.

**ELEKTROKİMYASAL YÖNTEM İLE SENTEZLENMİŞ NANOTEL ESASLI  
ELEKTROTLARIN ODAKLANMIŞ İYON DEMETİ İLE ÜRETİMİ**

**ÖZ**

200 nm çapında elektrokimyasal yöntem ile sentezlenmiş altın nanotelden açıklığı yaklaşık olarak 30 nm olan yeni nanoelektrotların üretimi gerçekleştirilmiştir. Açıklık  $10^{17}$  iyon /  $\text{cm}^2$  öğütme ve 0.2  $\mu\text{s}$  durma zamanı parametrelerinin kullanıldığı odaklanmış iyon demeti (FIB) ile sağlanmıştır. FIB ile öğütme öncesi ve havada devrenin boşluk aralığının I-V karakterizasyonu sonucu direncin sırasıyla 0.55 ile 4 G $\Omega$ , arasında olduğu belirlenmiştir.

**Anahtar Kelimeler:** Template sentezleme, Odaklanmış iyon demeti, Nano elektrot, Altın nanotel, Nano açıklık.

**1. INTRODUCTION**

Currently, one of the main challenges in nanotechnological structure development is to create reliable nanoelectrodes with a few nanometers spacing that can assess the electrical properties of individual nanoparticles for a variety of applications ranging from electronics to chemical and biological sensors.

Unfortunately many of the experimental electrode manufacturing techniques reported so far suffer from low yields in fabricating successful structures or from lack of the mechanical and electrical flexibility required for systematic in-

vestigation of charge transport characteristics (1,2).

One of the most successful approaches to fabricate a large number of nanowires (NWs) with high aspect ratio, that may form the basis for a new type of nanoelectrode, is the use of membrane-based templates for electrodeposition of multilayers as well as of single metals [3-5]. Template synthesis is an alternative to conventional lithography and enables the fabrication of ultra narrow NWs with a diameter down to less than 5 nm. Additionally, large varieties of NWs and nanotubes of ordered semiconductor arrays (Si, Ge, CdS, CdSe ZnO), metals (Cu, Co, Bi, Ni, Au), and metal oxides (Fe<sub>3</sub>O<sub>4</sub>, NiO,) can be

<sup>1</sup>Department of Engineering Sciences, The Ångström Laboratory, Uppsala University, Box 534, SE 751 21 Uppsala, Sweden

synthesized by using the template synthesis technique. Examples of such templates for electrodeposition of multilayers as well as single metallic NWs are the track-etched polycarbonate membrane (3,5), nanoporous aluminium oxide (6,7) and nanoporous mica (8).

Recently, we have reported that the Focused Ion Beam (FIB) technique can be used to form electrical contacts on a single Au NW [9-10]. The dual-beam FIB is equipped with Electron Beam Assisted Deposition (EBAD) and Ion Beam Assisted Deposition (IBAD) devices. IBAD and EBAD assisted deposition of Pt metal in our FIB/SEM system involve the decomposition of  $C_9H_{16}Pt$  gas molecules, resulting in the local deposition of Pt metal on the sample within the area where the ion beam is scanned. The mechanisms by which IBAD and EBAD function are similar, but the deposition efficiency for the IBAD process is much higher (11).

The present work reports on the fabrication of a new type of nanoelectrode constructed from electrochemically synthesized Au NWs that are lifted off and released between pre-patterned contact pads. The dual FIB deposition method is used to create interconnection bridges between the Au NW and the metallic contacts deposited on an oxidized silicon wafer. Thereafter, the full in-situ FIB method is exploited for milling a nano-sized gap in the NW.

## 2. EXPERIMENTAL METHOD

### 2.1. Electrochemical Synthesis of Au Nanowires

Au NWs were prepared by using the electrochemical synthesis technique inside nuclear-track-etched polycarbonate membranes with pores of 200 nm diameter serving as the template. Prior to the deposition of the Au NWs, the working electrode was fabricated by sputter depositing a 20 nm thick Ti layer followed by a 500 nm thick Au layer on one side of the membrane. The electrochemical fabrication process was performed using an EG&G Princeton Applied Research Model 263 potentiostat/galvanostat in a standard type three electrode electrolytic cell. A schematic illustration of the experimental arrangement is shown in Fig. 1. The electrodeposition of the Au NWs was performed at -690 mV in a standard gold electrolyte consisting of 0.8 M  $C_6H_8O_6$  and 0.003 M  $KAu(CN)_2$  at pH 3.5-4. The inset of Fig. 2 shows a SEM micrograph of Au NWs with an average length of approximately 20  $\mu m$

grown in the porous membrane after dissolving the membrane in dichloromethane ( $Cl_2CH_2$ ), and collecting the wires onto carbon grids.

### 2.2 In-situ Contacting and Milling of Nanostructures with The FIB Direct-Write Technique

The FIB/SEM system used was a FEI DB235. FIB/SEM is a combination of a high resolution 30 keV field emission gun SEM (FEGSEM) electron column (with spot sizes ranging from 2 to 10 nm) and a 30 keV  $Ga^+$  FIB column (with minimum beam spot size of 7 nm). The FIB column is tilted  $52^\circ$  with respect to the electron beam column. Both beams can be aligned to hit the same spot by eucentric height adjustment of the sample stage. The total beam density of  $Ga^+$  ions was set to  $10^{18}$  ions  $cm^{-2}$ . The FIB system is equipped with an injector through which trimethylmethylcyclopentadienyl-platinum ( $C_9H_{16}Pt$ ) gas molecules can be introduced near the sample surface. The gas molecules are then dissociated by one of the two beams and Pt metal is hence deposited on the sample surface. The operating parameters for the FIB during milling and deposition included an accelerating voltage of 30 kV, an emission current of 2.3  $\mu A$  and a dwell time of 0.1  $\mu s$  with 50% overlap at a chamber pressure of  $1.4 \times 10^{-6}$  mbar.

The Au NWs were dispersed on an oxidized Si wafer with Cr/Au pads. Figures 2 (a) to (c) show a FIB Omniprobe™ consisting of a tungsten needle used to extract an individual NW with a diameter of approximately 200 nm. In order to reduce the potential damage to the NW, Pt-EBAD deposition at a low acceleration electron energy of 3-5 kV and a reduced scan size was used to weld a single Au NW to the needle (Fig. 2 (a)). After welding, the attached NW was transferred close to the prepatterned four-point contact pads on the oxidized Si substrates (Fig. 2 (b)). Thereafter, the NW was released by making strategic cuts between the NW and the needle in order to place the NW in the desired position on the sample. Fig. 2 (c) shows the released NW in the middle of the prepatterned pads. Note that in Figs. 2 (a) and (b) the needle with the attached NW is above the substrate. Since the working distance is related to the substrate, the scaling bar does not describe the size of the probe or the NW in these figures. The contact bridges between the Au NW and the metallic contacts on the oxidized Si wafer were created using the dual FIB deposition method. The resistivity of the Au NW was found to be  $2.8 \times 10^{-4}$   $\Omega cm$  (10). After performing the resistivity measurements of the Au NW, the FIB was used to mill a nano-sized gap in a single Au NW in order to fabricate a novel NW based nanoelectrode device.

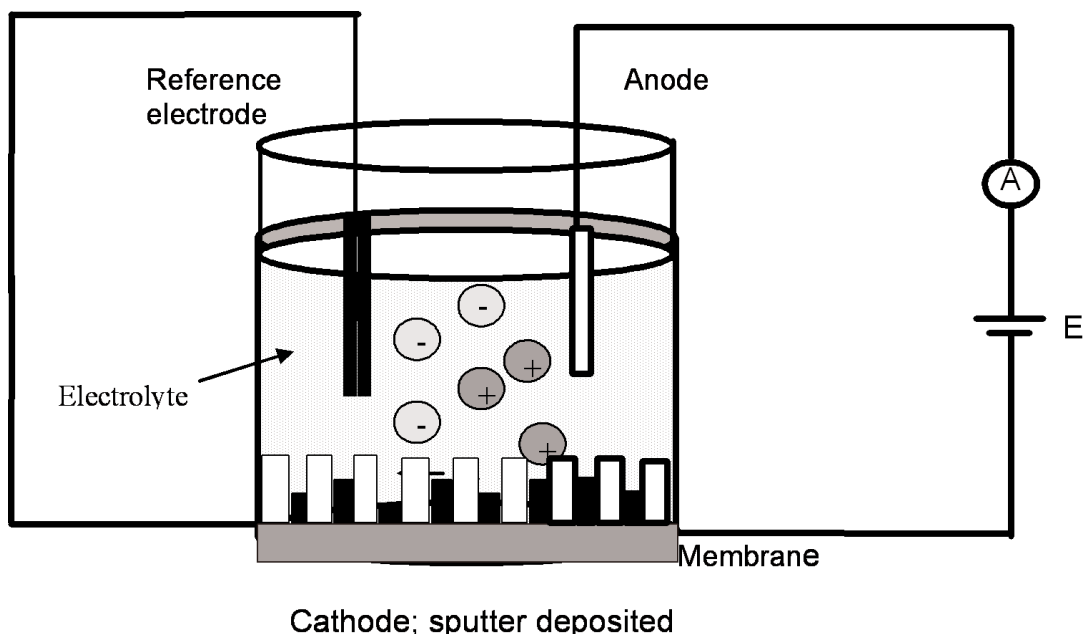


Figure.1. A schematic illustration of the experimental setup for template synthesis of Au NWs.

### 3. RESULTS AND DISCUSSION

#### 3.1 Fabrication and Characterization of the FIB-Milled Electrode Gaps

It is obvious that the interaction between the energetic ion beam and the NW will influence the properties of the fabricated nanogap. Additional to the optimal FIB processing parameters defined above, the ion dose and the dwell time are essential parameters that play a dominant role during the milling process. In order to investigate how to achieve a minimum gap size in the Au NW, ion beam currents ranging from 1 pA to 50 pA were investigated using a 0.1  $\mu$ s dwell time.

The results of the FIB milling yields for the cutting processes on the Au NW are given in Table 1 together with the obtained gap sizes. Figures 3 (a) to (c) show the topography of typical Au NWs cut by the FIB.

As seen in Fig. 3(a) at 50 pA, a gap of about 100 nm was milled and the gap shape showed a widening and narrowing effect at the top and bottom edges, respectively. The halo shape at the edge of the gap may originate from the non-Gaussian beam profile which causes a continuous re-deposition of sputtered material into the milled section.

A considerable improvement in the gap size and shape was observed at 30 pA. As seen in Fig. 3(b) the side wall of the gap is uniform with a smooth milled surface.

The influence of dwell time on the shape and size of the electrode gap was also investigated. Table 2 shows the gap size at different dwell times for a constant beam current of 1 pA. It can be noticed

that a minimum gap size of 30 nm with homogeneous spacing, as shown in Fig. 4, can be milled using a dwell time corresponding to 0.2  $\mu$ s. Changing the dwell time at a constant ion beam current has a crucial effect on the lateral gap size created in the NW because more material is milled away the longer the ion beam is fixed at a single position.

In order to test the possibility of using the nanoelectrode with 30 nm gap for transport studies, we perform an I-V measurement. The I-V response of the gap was recorded using a two-point probe connected to an Agilent B1500A Semiconductor Device analyzer. Fig. 5 shows I-V profiles recorded at 294 K on an Au NW before and after FIB milling. The I-V profiles of uncut and cut NWs showed ohmic behavior over the entire measurement range with resistances of 0.55 M $\Omega$  and 4.0 G $\Omega$ , respectively. The calculated resistance of the setup before FIB milling is in good agreement with our earlier study [9], with the Pt connections contributing to the major part of the resistance.

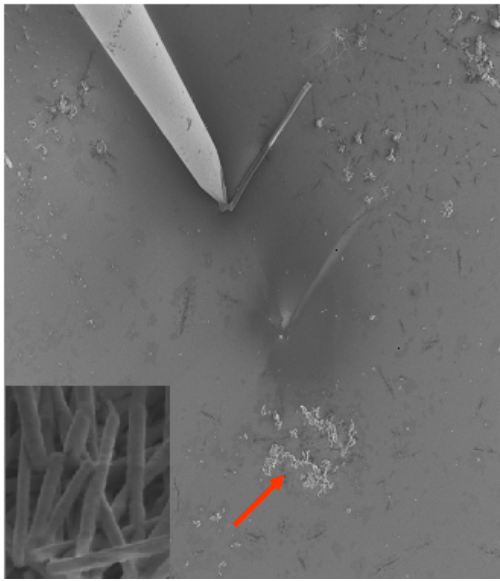


Figure.2a.

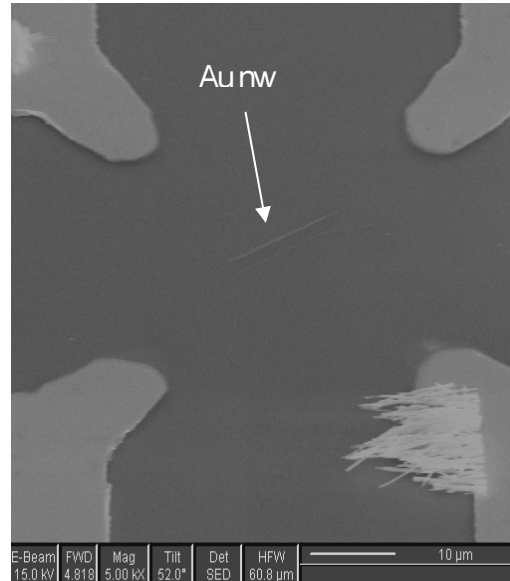


Figure.2b.

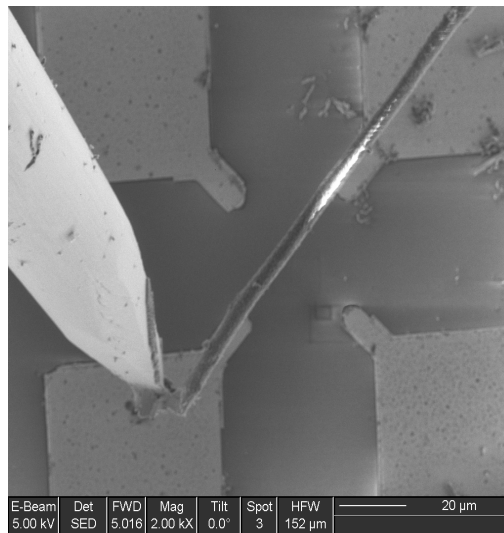


Figure .2c.

Figure 2. FIB/SEM images illustrating the four-contact nanoelectrode fabrication procedure using an Au NW. Panel (a) shows the NW welded in-situ by Pt-IBAD onto a nanomanipulator. The inset shows Au NWs with a diameter of 200 nm and an average length of  $20 \pm 3 \mu\text{m}$ , obtained from completely filled pores after dissolving the template membrane in dichloromethane ( $\text{Cl}_2\text{CH}_2$ ) and collecting the wires on carbon grids. Panel (b) shows the NW being transferred close to the prepatterned Au pads on the oxidized substrate inside the FIB. Panel (c) illustrates a NW released in the middle of the pads before contacting to the electrodes. Note that the working distance is related to the substrate. Thus, the scaling bars in panel (a) and (b) do not describe the correct size of the Omniprobe or the NW which are located above the substrate in these panels.

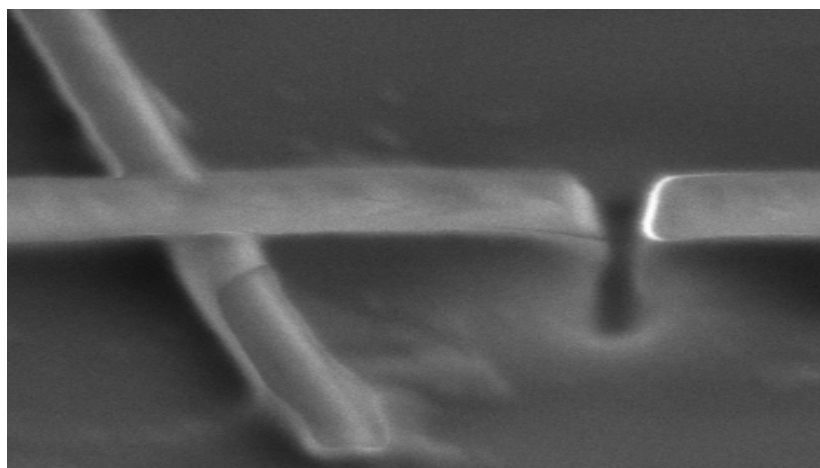


Figure 3. S. Valizadeh (a)

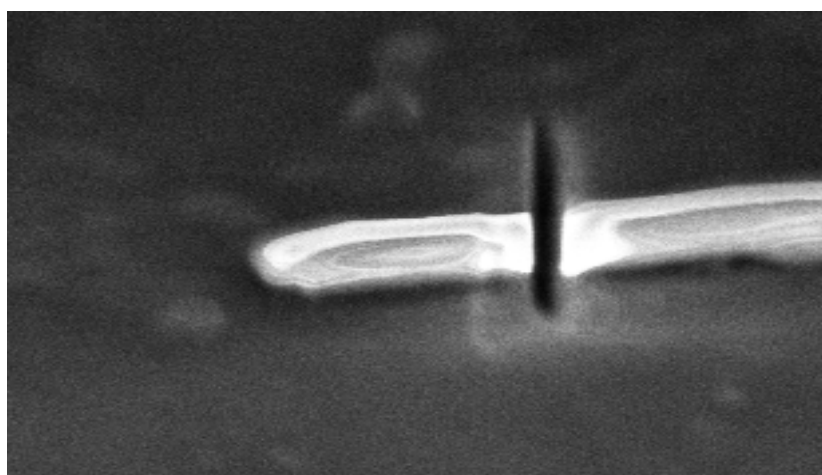


Figure 3(b).

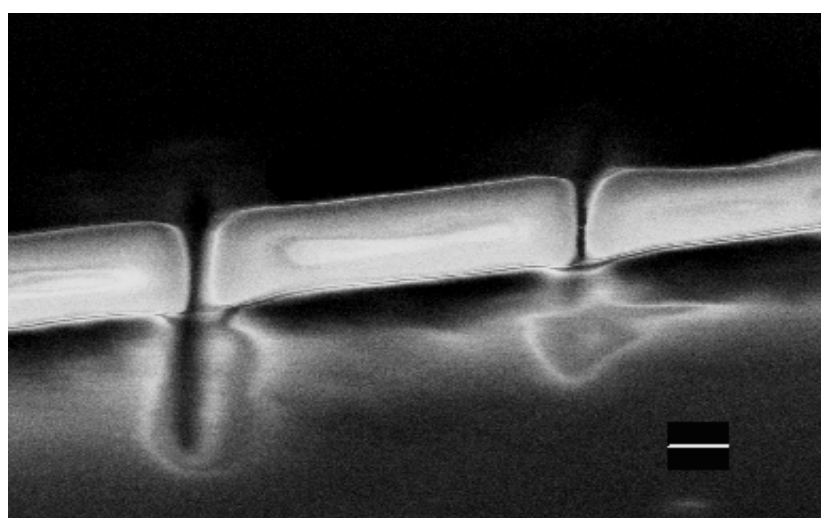


Figure 3(c).

Figure 3. FIB/SEM images of gaps milled in an Au NW by the FIB; the dwell time for the FIB milling processes was  $0.1 \mu\text{s}$ . Panel (a) shows a gap of 100 nm milled at 50 pA, (b) shows a gap of 80 nm milled at 30 pA, and (c) shows gaps of 50 nm and 35 nm milled at 10 pA and 1 pA, respectively.

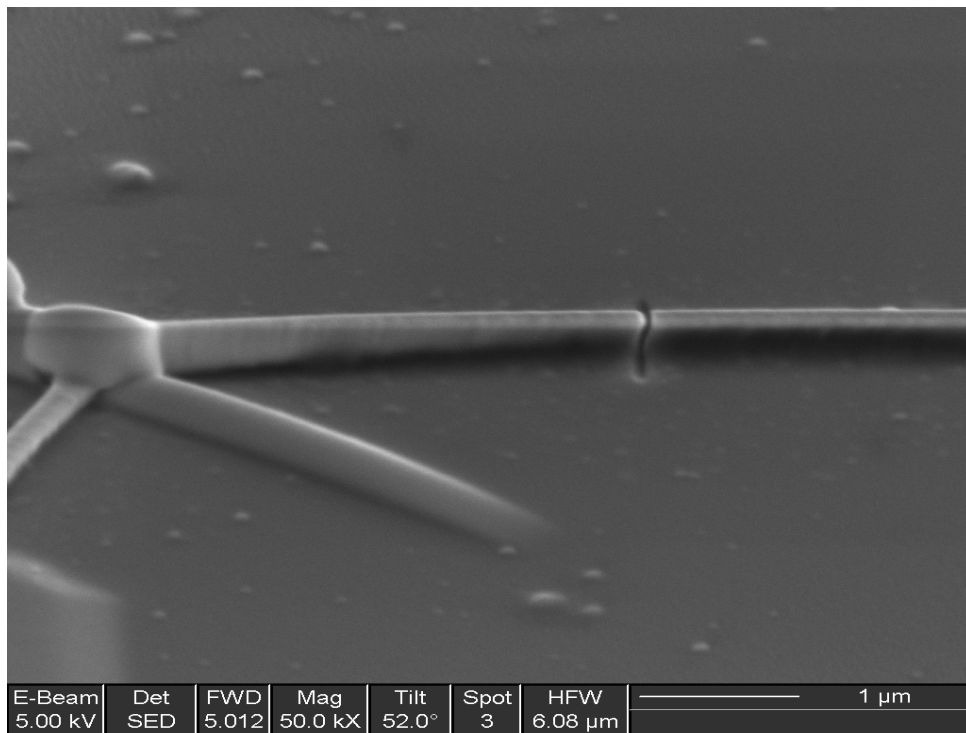


Figure 4. An illustration of the first prototype of the new Au NW based nanoelectrode. A gap of 30 nm was milled within the low dose regime of  $10^{17}$  ions /  $\text{cm}^2$  and a dwell time of  $0.2 \mu\text{s}$ . The SEM image is taken at a tilt angle of  $52^\circ$ .

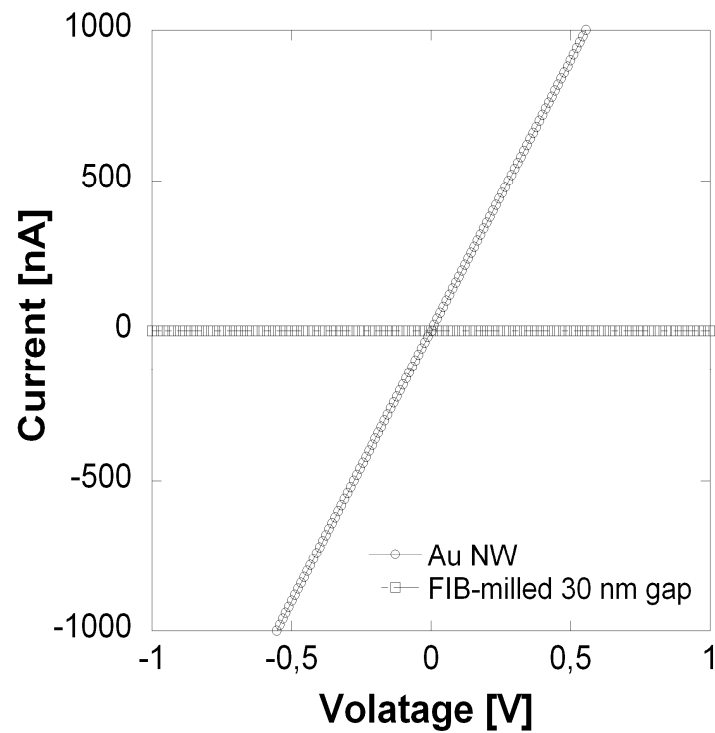


Figure 5. Current-voltage characteristics at 294 K for the nanoelectrode device of the Au NW prior to FIB milling and of the empty gap circuit in air. The displayed curves showed ohmic behavior with resistances of  $\sim 0.55 \text{ M}\Omega$  and  $\sim 4 \text{ G}\Omega$ , respectively.

Table 1. The results of FIB milling yield to create a minimum gap in Au NWs.

Ion beam current [pA]	Ion dose [ionscm <sup>-2</sup> ]	Gap size [nm]
1	6.11 x 10 <sup>17</sup>	35 ± 1
10	1.24 x 10 <sup>18</sup>	50 ± 2
30	1.25 x 10 <sup>18</sup>	80 ± 3
50	1.26 x 10 <sup>18</sup>	≥ 100

Table 2. Gap size evolution as a function of dwell time at a constant ion beam current of 1 pA. The uncertainty of the measured gap size is ± 1 nm.

Dwell time [μs]	Gap size [nm]
0.1	35
0.2	30
0.3	36
0.5	40

#### 4. CONCLUDING REMARKS

We have demonstrated a novel nanoelectrode fabrication technique based on in-situ manipulation and milling of NWs in a FIB/SEM chamber. The formation of 30 nm-sized electrode gaps in Au NWs was achieved by FIB milling in the low dose regime of 6.11 10<sup>17</sup> ions / cm<sup>2</sup> and using a dwell time of 0.2 μs. Thus, we have shown the potential of using electrochemically synthesized Au NWs in combination with the FIB technique, in order to make nanoelectronic devices with critical dimensions below 100 nm, using “top-down” fabrication techniques.

#### 5. ACKNOWLEDGEMENTS

Financial support from the Magnus Bergvalls and the Göran Gustafsson Foundations are gratefully acknowledged.

#### REFERENCES

- Nagase, T., Kubota, T., Mashiko, S. (2003). *Thin Solid Films*. 438-439, 374.
- Park, H., Lim, A.K.L., Alivisatos, A.P., Park, J. and McEuen, P.L. (1999). *Appl. Phys. Lett.* 75, 301.
- Valizadeh, S., George, J.M., Leisner, P. and Hultman, L. (2002). *Thin Solid Films*. 402, 262.
- Valizadeh, S., Leisner, P., Hultman, L. and George, J.M. (2002). *Adv. Functional Mater.* 11-12, 766.
- Valizadeh, S., George, J.M., Leisner, P. and Hultman, L. (2001). *Electrochim. Acta*. 47, 865.
- Valizadeh, S., George, J.M., Leisner, P. and Hultman, L. (2001). *Electrochim. Acta*. 47, 865 .
- Kashiwabara, S., Jyoko, Y. and Hayashi, Y. (1996). *Mat. Tran.* 37, 289.
- Cavallotti, P.L., Bozzini, B., Nobili, L. and Zangari, G. (1994). *Electrochimica Acta*. 39, 1123.
- Hernandez, F., Olga, O., Abid, M., Valizadeh, S., Rodriguez, J., Vila, A., Morante, J. and Romano-Rodriguez, R. (2005). *MRS Spring Meeting*.
- Valizadeh, S., Abid, M., Romano Rodriguez, A., Hjort, K. and Schweitz, J.A. (2006). *Nanotechnology*. 17, 1134.
- Stockman, L., Neuttiens, G., Van Haesendock, C. and Bruynseraede, Y. (1993). *Appl. Phys. Lett.* 62, 2935.
- Chyr, C. Chao and Steckl, A.J. (1999). *J. Vac. Sci. Technol. B* 17, 3063.
- Frey L. and Ryssel, C.L.H. (2003). *Applied Physics. A* 76, 1017.
- Templeton M. and H. Champion, H.G. (1995). *J. Vac. Sci. Technol. B* 13, 2603.



**Sima VALIZADEH**, She received a B.Sc. in Physics, Chemistry and Mathematic in 1983 in Mysore University of India, 1992 B.Sc. in Physics in Linköping University in Sweden and PhD on Electrodeposition on Compositionally Modulated Thin Films and Nanowire Arrays, at Thin

film physics division in Linköpings University  
in Sweden in 2001.